

The quantum nature of light in high harmonic generation

Maciej Lewenstein,^{1,2*} Marcelo F. Ciappina,^{1,3} Emilio Pisanty,¹
Javier Rivera-Dean,¹ Theocharis Lamprou,^{4,5} and Paraskevas Tzallas^{4,6*}

¹ICFO - Institut de Ciencies Fotoniques, The Barcelona Institute of Science and Technology,
08860 Castelldefels (Barcelona), Spain

²ICREA, Pg. Lluís Companys 23, 08010 Barcelona, Spain

³Institute of Physics of the ASCR, ELI-Beamlines project, Na Slovance 2,
182 21 Prague, Czech Republic

⁴Foundation for Research and Technology-Hellas, Institute of Electronic Structure & Laser,
GR-70013 Heraklion (Crete), Greece

⁵Department of Physics, University of Crete, P.O. Box 2208,
GR-71003 Heraklion (Crete), Greece

⁶ELI-ALPS, ELI-Hu Non-Profit Ltd., Dugonics tr 13, H-6720 Szeged, Hungary

*To whom correspondence should be addressed;
E-mail: maciej.lewenstein@icfo.eu and ptzallas@iesl.forth.gr

High-harmonic generation is one of the most fundamental processes in strong laser-field physics that has led to countless achievements in atomic physics and beyond. However, a rigorous quantum electrodynamical picture of the process has never been reported. Here, we prove rigorously and demonstrate experimentally that the quantum state of the driving laser field, as well as that of harmonics, is coherent. Projecting this state on its part corresponding to harmonic generation, it becomes a superposition of a state, amplitude-shifted due

to the quantum nature of light, and the initial state of the laser. This superposition interpolates between a Schrödinger "kitten", and a genuine Schrödinger "cat" state. This work opens new paths for ground-breaking investigations in strong laser-field physics and quantum technology. We dedicate the work to the memory of Roy J. Glauber, the inventor of coherent states.

High harmonic generation (HHG) is at the heart of attosecond science (*1*) and it is hard to overestimate its fundamental and technological importance (for reviews in the recent decades see (*2–5*)). HHG has been in the center of interest of atomic, molecular and optical (AMO) physics, as well as laser physics since 1988 (*6, 7*). The understanding of this process was boosted from the formulation of the three-step, or simple man's model (*8, 9*), and its quantum version (*10*). In this approach, HHG from a single atom/molecule/solid, is initiated by electron's tunnelling to the continuum, its subsequent acceleration in the intense laser field, and finally its recombination to the ground state of the target. With respect to the electrons, this process is evidently quantum: it involves their *quantum tunneling, wave packet evolution, and recombination*. On the other hand, it is usually described in a semiclassical way with respect to the driving laser field: the argument is that it is a strong coherent field, and its quantum depletion effects are small. The quantum nature of harmonic photons is usually also neglected: one calculates the HHG spectrum simply via Fourier transform of the electronic time-dependent dipole moment (or more precisely the dipole acceleration). This quantity is then used to calculate the spatial-propagated harmonics and the extremely subtle and important phase matching conditions (*2*).

The question of quantum nature and quantum properties of HHG has been “in the air” for some time. Several groups attempted to study this problem theoretically (*11–14*) and experi-

mentally (15, 16). In its simplest version, this question has two facets: I) what is the quantum depletion of the fundamental laser mode? and II) what is the quantum state of the generated harmonics?

In this report we answer these two questions. We prove rigorously that if the initial state of the system of N atoms in their ground states is impinged by a laser in a coherent state of amplitude α_L , then the quantum state of the laser mode and the harmonic modes are coherent. We determine this exactly. However, due to coherences and correlations between the fundamental laser and harmonics modes, the laser mode amplitude is shifted by $\alpha_L \rightarrow \alpha_L + \delta\alpha_L$. Hence, the final state of the laser mode, conditioned on harmonic generation, is a superposition of the two coherent states: the initial and the shifted one. This state interpolates between a Schrödinger “kitten” state, corresponding to a coherently shifted first Fock state (for small $\delta\alpha_L$), and a genuine Schrödinger “cat” state (for $\delta\alpha_L$ comparable with α_L). We exactly calculate $\delta\alpha_L$, as well as the coherent amplitudes of the harmonics. The above results are confirmed experimentally by characterizing the quantum state of the light field exiting a gas phase HHG medium, when the state is conditioned to the HHG. This has been achieved by combining the Quantum Tomography (QT) approach (17) with a photon correlation method, namely Quantum Spectrometer (QS) (15, 16).

Of course, the theoretical approach relies in several simplifying assumptions, but all of them can be avoided using reasonable approximations. For instance, the reason why we can achieve these results is because we condition our analysis on the electrons being in or back in the ground state, “ignoring” in a sense the electrons being ionized. Also, in order to describe a laser pulse with a given envelope, one needs a continuum of photon modes contributing to this wave packet. We avoid this complexity by multiplying the atom-field interaction Hamiltonian by an envelope function $f(t)$, in some analogy to scattering theory in many body quantum field theories. Our

starting point is then the time-dependent Schrödinger equation

$$i\hbar \frac{\partial}{\partial t} |\tilde{\Psi}(t)\rangle = \hat{H} |\tilde{\Psi}(t)\rangle, \quad (1)$$

where the Hamiltonian, \hat{H} , describes the laser-target system in single electron approximation (SAE), and is the sum of three terms, i.e. $\hat{H} = \hat{H}_0 + \hat{U} + \hat{H}_f$ where $\hat{H}_0 = \frac{\hat{\mathbf{p}}^2}{2m} + V(\hat{\mathbf{r}})$ is the laser-free Hamiltonian of the atomic or molecular system with $V(\hat{\mathbf{r}})$ being the effective SAE atomic or molecular potential, m the electron mass, and $\hat{U} = -e\hat{\mathbf{E}} \cdot \hat{\mathbf{r}}$ the dipole coupling, which describes the interaction of the atomic or molecular system with the laser radiation, written in the length gauge, and under the dipole approximation.

In principle, to describe laser/harmonic pulses of finite duration and spatial extension, the full continuum spectrum of the electromagnetic (EM) field must be considered. Here, we simplify the Hamiltonian to a sum of effective discrete modes. The free EM field Hamiltonian reduces in our case to

$$\hat{H}_f = \hbar\omega \hat{a}^\dagger \hat{a} + \sum_q^{cutoff} \hbar\omega q \hat{b}_q^\dagger \hat{b}_q, \quad (2)$$

where \hat{a}^\dagger , \hat{a} , \hat{b}_q^\dagger , \hat{b}_q are creation (annihilation) operators of the laser and harmonic modes, respectively. To account for finite pulse duration we model the electric field operator as

$$\hat{\mathbf{E}} = -i\hbar \mathbf{g}(\omega_L) f(t) \left[(\hat{a}^\dagger - \hat{a}) + \sum_3^{cutoff} \sqrt{q} (\hat{b}_q^\dagger - \hat{b}_q) \right]. \quad (3)$$

In Eq. (3) the dimensionless function $0 \leq f(t) \leq 1$ describes the envelope of the laser pulse normalized to one at maximum. We denote the effective coefficient entering into the expansion of the electric field into the modes by $\mathbf{g}(\omega) \propto \sqrt{\omega/V_{eff}}$, where V_{eff} is the effective quantization volume (18, 19). $e\mathbf{g}(\omega)$ encodes information about the polarization of the modes, and has the dimension [1/m/sec], and for the typical frequencies used in strong field physics is very small, on the order of 10^{-8} in a. u..

Equation (1) needs to be solved subject to the initial condition $|\tilde{\Psi}(0)\rangle = |g, \alpha_L, \Omega_H\rangle$, i.e. for the electron initially in its ground state $|g\rangle$, the laser in a coherent state $|\alpha_L\rangle$, and the harmonics in the vacuum state $|\Omega_H\rangle$. To this aim we write $|\tilde{\Psi}(t)\rangle = D(\alpha_L) \exp(-i\hat{H}_ft/\hbar)|\Psi(t)\rangle$, where $D(\alpha_L)$ is the Glauber's shift operator creating a coherent state $|\alpha_L\rangle$ from the vacuum of the laser mode, $|\Omega_L\rangle$. The second unitary operator transforms to the interaction picture with respect to the EM field. Then, we obtain

$$i\hbar \frac{\partial}{\partial t} |\Psi(t)\rangle = [\hat{H}_{sc} - e\hat{\mathbf{E}}_Q(t) \cdot \hat{\mathbf{r}}] |\Psi(t)\rangle, \quad (4)$$

where $\hat{H}_{sc}(t) = \hat{H}_0 - e\mathbf{E}_L(t) \cdot \hat{\mathbf{r}}$ while $\mathbf{E}_L(t) = -i\hbar|\mathbf{g}(\omega_L)|f(t)[\alpha_L^*e^{i\omega_L t} - \alpha_L e^{-i\omega_L t}]$ is the “classical” electric field of the laser pulse. The quantum correction is

$$\begin{aligned} \hat{\mathbf{E}}_Q(t) &= -i\hbar\mathbf{g}(\omega_L)f(t) \left[\hat{a}^\dagger e^{i\omega_L t} - \hat{a} e^{-i\omega_L t} \right. \\ &\quad \left. + \sum_{q=3}^{cutoff} \sqrt{q} [\hat{b}_q^\dagger e^{iq\omega_L t} - \hat{b}_q e^{-iq\omega_L t}] \right]. \end{aligned} \quad (5)$$

Note that the initial condition for $|\Psi(t)\rangle$ is $|\Psi(0)\rangle = |g, \Omega_L, \Omega_H\rangle$. The next step is to go to the interaction picture with respect to $\hat{H}_{sc}(t)$, $|\Psi(t)\rangle = \mathcal{T} \exp[-i \int_0^t \hat{H}_{sc}(t') dt'/\hbar] |\psi(t)\rangle$, where \mathcal{T} denotes the time ordered product. Then we obtain:

$$i\hbar \frac{\partial}{\partial t} |\psi(t)\rangle = -e\hat{\mathbf{E}}_Q(t) \cdot \hat{\mathbf{r}}_H(t) |\psi(t)\rangle. \quad (6)$$

The initial condition remains the same, while $e\hat{\mathbf{r}}_H(t)$ denotes the time-dependent dipole operator in the Heisenberg picture with respect to \hat{H}_{sc} . The electron might be, due to this evolution, ionized in the continuum (above threshold ionization process, ATI), or (hardly) remains in some bound excited states. Most of the physics relevant for HHG happens in the ground state: whatever remains there, remains there; whatever recombines to it, is related to a harmonic emission. Therefore, it makes sense to condition Eq. (6), upon neglecting of the (small) continuum/excited part of $|\psi(t)\rangle$, on the ground state, i.e. consider $|\phi(t)\rangle = \langle g|\psi(t)\rangle$, which fulfills

$$i\hbar \frac{\partial}{\partial t} |\phi(t)\rangle = -\hat{\mathbf{E}}_Q(t) \cdot \langle \hat{\mathbf{d}}_H(t) \rangle |\phi(t)\rangle. \quad (7)$$

The above equation constitutes one of our main results: it rigorously describes the evolution of the state of the laser and harmonic modes, conditioned on the atomic ground state.

Note that $\langle \hat{\mathbf{d}}_H(t) \rangle$ is the quantum averaged time-dependent dipole moment, that can be easily calculated solving the time-dependent Schrödinger equation (TDSE), or even easier using the strong field approximation (SFA) (cf. (5, 10)). Also, the effective Hamiltonian $\hat{H}_Q(t) = -\hat{\mathbf{E}}_Q(t) \cdot \langle \hat{\mathbf{d}}_H(t) \rangle$ is a linear form of photon creation and annihilation operators. Thus, the unitary evolution operator is an exponent of a linear form of creation and annihilation operators, and as such when acting on coherent states, it will simply shift them. One can obviously calculate exactly the evolution operator corresponding to $\hat{H}_Q(t)$. Since $[\hat{H}_Q(t), \hat{H}_Q(t')] = c(t - t')$ is simply a complex number, this is trivially achieved applying multiple times the Baker-Campbell-Hausdorff formula. The final result (up to an uninteresting prefactor) at time T after termination of the laser pulse, and after returning to the “laboratory” frame is:

$$|\phi(t)\rangle = |\alpha_L + \delta\alpha_L e^{-i\omega_L T}, \beta_3 e^{-3i\omega_L T}, \dots, \beta_q e^{-qi\omega_L T}, \dots\rangle, \quad (8)$$

where $\delta\alpha_L = -ig(\omega_L) \cdot \mathbf{d}_{\omega_L}$, and $\beta_q = -ig(\omega_L) \sqrt{q} \cdot \mathbf{d}_{q\omega_L}$. Here, $\mathbf{d}_\omega = \int_0^T f(t) e^{i\omega t} \langle \hat{\mathbf{d}}_H(t) \rangle$, is a Fourier transform of the time averaged semiclassical dipole moment, “tempered” with respect to the pulse envelope. Assuming that N atoms contribute to HHG coherently in a phase matched way we obtain the final, main result. The state of the laser and harmonic fields after the pulse is coherent with

$$\delta\alpha_L = -iN\mathbf{g}(\omega_L) \cdot \mathbf{d}_{\omega_L}, \quad (9)$$

$$\beta_q = -iN\mathbf{g}(\omega_L) \sqrt{q} \cdot \mathbf{d}_{q\omega_L}. \quad (10)$$

The above rigorous and analytic expressions constitute the main results of this paper.

In the seminal experiments presented below, the tomography of the fundamental laser mode is performed after two steps. The first consists in reducing the amplitude of this mode by a

factor $\cos(r)$. In this way, $\alpha_L \rightarrow \cos(r)\alpha_L = \alpha$, $\delta\alpha_L \rightarrow \cos(r)\delta\alpha_L = \delta\alpha$. The second step corresponds to conditioning on HHG, i.e. post-selection of the part of the state that includes at least one harmonic photon. Mathematically it means that

$$\begin{aligned} |\alpha + \delta\alpha\rangle &\rightarrow (1 - |\alpha\rangle\langle\alpha|)|\alpha + \delta\alpha\rangle \\ &= |\alpha + \delta\alpha\rangle - \langle\alpha|\alpha + \delta\alpha\rangle|\alpha\rangle. \end{aligned} \quad (11)$$

It is elementary to see that the state is a superposition of the two coherent states, so it is a Schrödinger "cat" state, similar to those measured in the seminal experiments by Haroche *et al.* (20, 21). However, if the two coherent states are very close one to another, this is a "kitten" rather than a genuine cat. In fact, we obtain two limiting cases:

I) If $|\delta\alpha/\alpha| \ll 1$, then the post-selected state $|\phi_{\text{post}}\rangle$, conditioned on HHG, is nevertheless quite non-classical, corresponding to a shifted Fock state,

$$|\phi_{\text{post}}\rangle = (\hat{a}^\dagger - \alpha^*)|\alpha\rangle.$$

having a Wigner function $W(\beta) = (4|\beta - \alpha|^2 - 1)e^{-|\beta - \alpha|^2/2}$ (Fig. 1 A, B) and a photon number distribution $p_n = |n/\alpha - \alpha^*|^2|\alpha|^{2n} \exp(-|\alpha|^2)/n!$.

II) If $|\delta\alpha| \simeq |\alpha|$ the state $|\phi_{\text{post}}\rangle$ corresponds indeed to a genuine Schrödinger cat state, depicting a Wigner function $W(\beta) = e^{-2|\beta - \alpha - \delta\alpha|^2} + e^{-|\delta\alpha|^2}e^{-2|\beta - \alpha|^2} - (e^{2(\beta - \alpha)\delta\alpha^*} + e^{2(\beta - \alpha)^*\delta\alpha})e^{-|\delta\alpha|^2}e^{-2|\beta - \alpha|^2}$ (Fig. 1 C, D) with negative regions (cf. (23)) and a photon number distribution $p_n = |(\alpha + \delta\alpha)|^n \exp(-|\alpha + \delta\alpha|^2/2) - \langle\alpha|\alpha + \delta\alpha\rangle\alpha^n \exp(-|\alpha|^2/2)|^2/n!$.

The experimental results, discussed with more detail below, suggest that experiment corresponds indeed to the second case of genuine Schrödinger "cat" state. Since $\alpha_L \simeq 10^6$, that would require that $N\mathbf{g}(\omega_L) \cdot \mathbf{d}_{\omega_L} \simeq 10^6$. We expect that the atomic dipole moment is of the order of e times the electron excursion amplitude, that is 10-100 a.u.. That would imply that the number of atoms participating in the coherent, phase matched HHG is $N \simeq 10^{12} - 10^{13}$, which agrees very well with experimental estimations (see Supplementary Material (SM)).

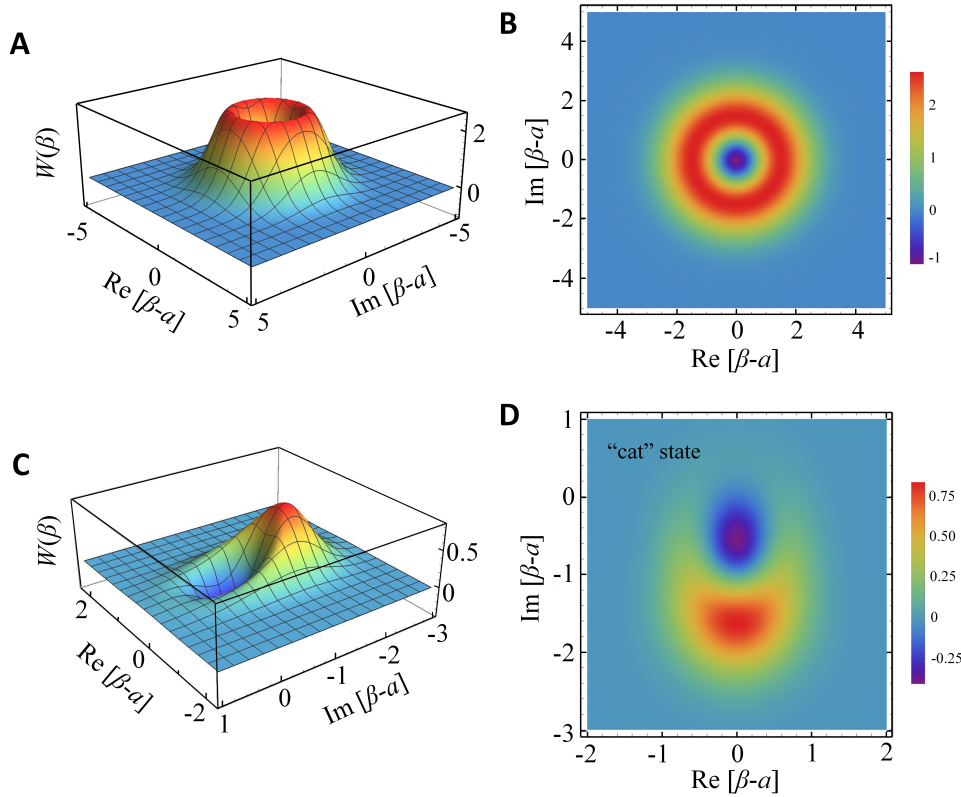


Figure 1: Calculated Wigner functions of a Schrödinger ‘kitten’ and a genuine Schrödinger ‘cat’ state. (A) Wigner function of a Schrödinger ‘kitten’ state, corresponding to coherently shifted first Fock state for small $\delta\alpha$. (B) Projection on the $(Re[\beta - \alpha], Im[\beta - \alpha])$ plane. (C) Wigner function of a genuine Schrödinger ‘cat’ state for $|\delta\alpha| = 1.5$ comparable with $|\alpha| = 2$. It is noted that the exact shape of the Wigner function depends on the ratio $|\delta\alpha/\alpha|$. (D) Projection on the $(Re[\beta - \alpha], Im[\beta - \alpha])$ plane. Here, we have used a ratio which provides a function reasonably close to the experimental results. The Wigner functions were plot according to the terminology of ref. (22))

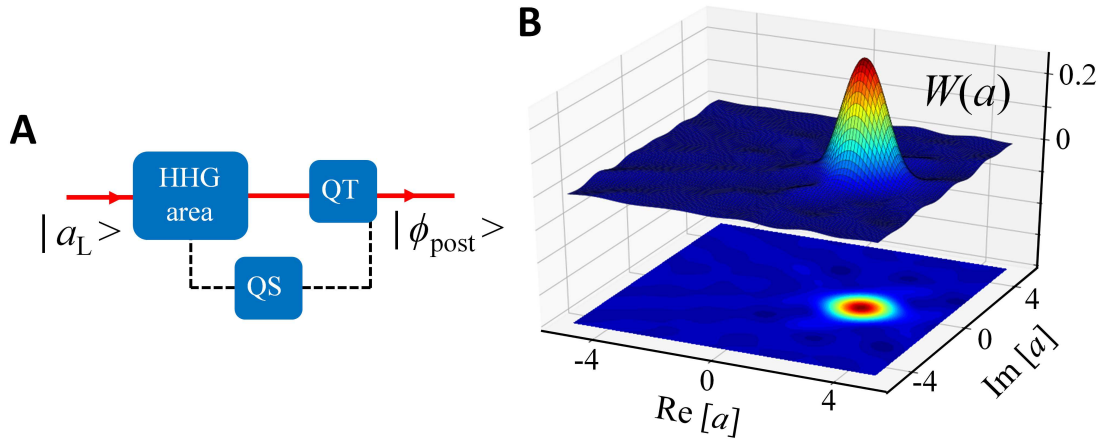


Figure 2: Experimental approach and measurement of the Wigner function of the coherent state of the driving laser field. (A) Schematic of the experimental set-up showing the HHG area, the QT approach, the QS, the coherent state of the driving IR laser field $|\alpha_L\rangle$ and, the conditioned to HHG, state of the IR light field exiting the medium $|\phi_{post}\rangle$. (B) Wigner function of the coherent state of the driving IR laser field measured when the HHG process was switched off.

The experiment has been performed using the set-up shown schematically in Fig. 2A. The arrangement consists of the HHG area, the QT approach, and the QS. The QT was used to completely characterize the quantum state of the light field exiting the atomic medium, and the QS to condition the outgoing from the medium light state with HHG process. The harmonics were generated by focusing a linearly polarized ≈ 35 fs infrared (IR) laser pulse with mean photon number $\approx 2 \times 10^{14}$ photons per pulse into a Xenon gas jet (for details see SM). As was expected, when the HHG process was switched off (Xenon gas jet off) the state of the driving IR laser field is coherent depicting a Wigner function with Gaussian distribution (Fig. 2B). When the HHG process was switched on (Xenon gas jet on) the state of the IR light field (conditioned to the HHG) exiting the gas, in agreement with the theoretical predictions, clearly shows the presence of the genuine Schrödinger “cat” state, (Fig. 3A, B).

Finally, another interesting observation is that the harmonic emission and the shift of the coherent state of the fundamental mode are correlated. Indeed, the whole process is governed

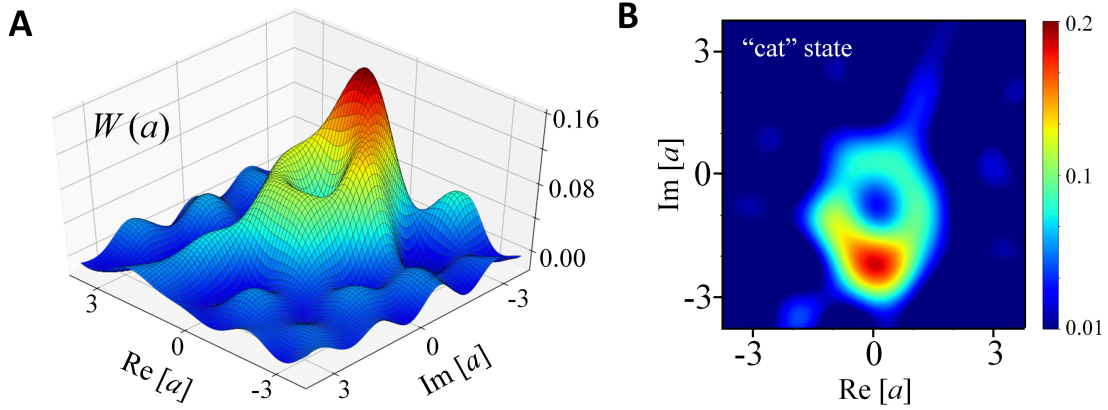


Figure 3: Measurement of the Wigner function of the genuine Schrödinger ‘‘cat’’ state. (A) Measured Wigner function of the light field conditioned to the HHG. In agreement with the theoretical predictions, the function clearly shows a genuine Schrödinger ‘‘cat’’ state. (B) Contour color plot of the projected Wigner function on the $(Re[\alpha], Im[\alpha])$ plane.

by a ‘‘wave packet’’ mode described by a creation operator:

$$\hat{B}^\dagger(t) \propto \hat{a}^\dagger e^{i\omega_L t} + \sum_{q=3}^{cutoff} \sqrt{q} \hat{b}_q^\dagger e^{iq\omega_L t}. \quad (12)$$

Note that the global coherent state is a product state, but only the effective mode described by Eq. (12) is excited-shifted; all other, orthogonal model remain unaffected. Of course, the parts corresponding to the fundamental and the harmonics oscillate at very different frequencies, and thus the observation of such correlations requires the implementation of approaches, like RABBIT or streaking (*I*), that can provide attosecond time resolution.

Our findings benchmark the birth of a novel research field composed by the two major research domains of strong field physics and quantum optics. Evidently, processes induced in strongly laser driven materials lead to novel classes of quantum states of light, including genuine Schrödinger ‘‘cat’’ states. The high level of quantumness, and dependence of these states upon the generation conditions, promises fascinating applications in quantum metrology and sensing.

References and Notes

1. F. Krausz and M. Y. Ivanov, *Rev. Mod. Phys.*, **81**, 163-234 (2009).
2. P. Salières, A. L'Huillier, Ph. Antoine, and M. Lewenstein, *Study of spatial and temporal coherence of high order harmonics* (Adv. At. Mol. Opt. Phys., volume 41, pages 83-142. Academic Press, 1999).
3. M. Lewenstein and A. L'Huillier, *Principles of Single Atom Physics: High-Order Harmonic Generation, Above-Threshold Ionization and Non-Sequential Ionization* (Strong Field Laser Physics, pages 147-183. Springer, New York, 2009).
4. G. Vampa and T. Brabec, *J. Phys. B: At. Mol. Opt. Phys.*, **50**, 083001, (2017).
5. K. Amini, J. Biegert, F. Calegari, A. Chacón, M. F. Ciappina, A. Dauphin, D. K. Efimov, C. F. de M. Faria, K. Giergiel, P. Gniewek, A. S. Landsman, M. Lesiuk, M. Mandrysz, A. S. Maxwell, R. Moszyński, L. Ortmann, J. A. Pérez-Hernández, A. Picón, E. Pisanty, J. Prauzner-Bechcicki, K. Sacha, N. Suárez, A. Zaïr, J. Zakrzewski, and M. Lewenstein, *Rep. Prog. Phys.*, **82**, 116001 (2019).
6. A. McPherson, G. Gibson, H. Jara, U. Johann, T. S. Luk, I. A. McIntyre, K. Boyer, and C. K. Rhodes, *J. Opt. Soc. Am. B*, **4**, 595601 (1987).
7. M. Ferray, A. L'Huillier, X. F. Li, L. A. Lompré, G. Mainfray, and C. Manus, *J. Phys. B: At. Mol. Opt. Phys.*, **21**, L31 (1988).
8. P. B. Corkum, *Phys. Rev. Lett.*, **71**, 1994-1997 (1993).
9. K. C. Kulander, K. J. Schafer, and J. L. Krause, *Dynamics of short-pulse excitation, ionization and harmonic conversion*, (Super-Intense Laser Atom Physics, volume 316 of NATO Advanced Studies Institute Series B: Physics, pages 95-110, Plenum, New York, 1993).

10. M. Lewenstein, Ph. Balcou, M. Yu. Ivanov, A. L’Huillier, and P. B. Corkum, *Phys. Rev. A*, **49**, 2117-2132 (1994).
11. D. J. Diestler, *Phys. Rev. A*, **78**, 033814 (2008).
12. I. A. Gonoskov, N. Tsatrafyllis, I. K. Kominis, and P. Tzallas, *Sci. Rep.*, **6**, 32821 (2016).
13. Á. Gombkötő, S. Varró, P. Mati, and P. Földi, *Phys. Rev. A*, **101**, 013418 (2020).
14. A. Gorlach, O. Neufeld, N. Rivera, O. Cohen, and I. Kaminer, *arXiv:1910.13791* (2019).
15. N. Tsatrafyllis, I. K. Kominis, I. A. Gonoskov, and P. Tzallas, *Nat. Commun.*, **8**, 15170 (2017).
16. N. Tsatrafyllis, S. Kühn, M. Dumergue, P. Földi, S. Kahaly, E. Cormier, I. A. Gonoskov, B. Kiss, K. Varju, S. Varro, and P. Tzallas, *Phys. Rev. Lett.*, **122**, 193602 (2019).
17. G. Breitennbach, S. Schiller, and J. Mlynek, *Nature* **387**, 471 (1997).
18. A. Wünsche, *J. Opt. B: Quantum Semiclass. Opt.*, **6**, S47-S59 (2004).
19. G. Grynberg, A. Aspect, and C. Fabre, *Introduction to Quantum Optics* (Cambridge University Press, Cambridge, 2010).
20. M. Brune, S. Haroche, J. M. Raimond, L. Davidovich, and N. Zagury, *Phys. Rev. A*, **45**, 5193 (1992).
21. S. Deléglise, I. Dotsenko, C. Sayrin, J. Bernu, M. Brune, J. M. Raimond, and S. Haroche, *Nature*, **455**, 510-514 (2008).
22. A. Royer, *Phys. Rev. A*, **15**, 449 (1976).
23. W. P. Schleich, *Quantum Optics in Phase Space* (Wiley-VHC Verlag, Berlin, 2001).

Acknowledgments

We thank Jens Biegert, Ido Kaminer, and Pascal Salières for enlightening discussions. We also Prof. S. Karsch from Max Plank Institute for Quantum Optics for his assistance on maintaining the performance of the Ti:Sa laser system and N. Pappadakis for his contribution on the development of the data acquisition and data analysis system. **Funding:** M.L. group acknowledges ERC AdG NOQIA, Spanish Ministry MINECO and State Research Agency AEI (FIDEUA PID2019-106901GB-I00/10.13039 / 501100011033, SEVERO OCHOA No. SEV-2015-0522 and CEX2019-000910-S, FPI), European Social Fund, Fundaci Cellex, Fundaci Mir-Puig, Generalitat de Catalunya (AGAUR Grant No. 2017 SGR 1341, CERCA program, QuantumCAT_U16-011424 , co-funded by ERDF Operational Program of Catalonia 2014-2020), MINECO-EU QUANTERA MAQS (funded by State Research Agency (AEI) PCI2019-111828-2 / 10.13039/501100011033), EU Horizon 2020 FET-OPEN OPTOLogic (Grant No 899794), and the National Science Centre, Poland-Symfonia Grant No. 2016/20/W/ST4/00314. M. F. C. acknowledges the Grantov agentura Cesk Republiky (GACR Grant 20-24805J). J.R-D. has received funding for this project from Secretaria d'Universitats i Recerca de la Generalitat de Catalunya and the European Social Fund. P.T. group acknowledges LASERLABEUROPE (ECs Seventh Framework Programme Grant No.284464), FORTH Synergy Grant AgiIDA, HELLAS-CH (MIS Grant No. 5002735) [which is implemented under the Action for Strengthening Research and Innovation Infrastructures, funded by the Operational Program Competitiveness, Entrepreneurship and Innovation (NSRF 20142020) and co-financed by Greece and the European Union (European Regional Development Fund)], and the European Unions Horizon 2020 research. ELI-ALPS is supported by the European Union and co-financed by the European Regional Development Fund (GINOP Grant No. 2.3.6-15-2015-00001). **Author contributions:** M. L.: Supervised the theoretical part of the work; M. F. C., J. R-D, E. P.:

equally contributed to the development of the theoretical approach; Th. L.: contributed in the experimental runs and data analysis; P. T.: Supervised the experimental part of the work.

Supplementary materials

The optical layout of the set-up is shown in Fig. 4. The measurement was performed using a linearly polarized ≈ 35 fs Ti:Sapphire laser pulse of $\lambda \approx 800$ nm carrier wavelength and an interferometer. The whole system was operating at 0.5 kHz repetition rate i.e. a single measurement of the quadrature was recorded in each laser shot. The IR laser beam was passing through a beam splitter BS_1 , having 80% transmission and 20% reflection. In the 1st branch of the interferometer, an ≈ 6 mm diameter IR beam (IR_t) with mean photon number $\approx 2 \times 10^{14}$ photons per pulse was focused by means of an 15 cm focal length lens (L1) into ≈ 1.2 mm long Xenon pulsed gas jet where the strong-field laser-atom interaction and HHG process was taking place. In order to avoid ionization saturation effects and minimize the distortions of the driving laser-field during the propagation in Xenon gas, the intensity of the IR_t beam in the interaction region was kept below $\approx 10^{14}$ W/cm². Also, in this configuration the confocal parameter is more than twice longer than the medium length and thus the intensity of the laser beam along the propagation in Xenon gas can be considered constant. A rough estimation of the number of atoms participating in the HHG process can be obtained by considering that in realistic experimental conditions of an interaction volume in the range of $10^{-5} - 10^{-6}$ cm³, and an atomic density $\sim 10^{18}$ atoms/cm³. In this case the number of atoms participating in the HHG process is in the order of $\sim 10^{13}$ atoms. Also, considering a tunneling ionization probability of $\sim 5\%$ it can be roughly estimated that the number of IR photons contributed to the HHG is $\sim 10^{12}$.

The IR field exiting the Xenon gas and the emitted high-harmonics were entered the QS which was used to disentangle the quantum electrodynamics of the high-harmonic generation

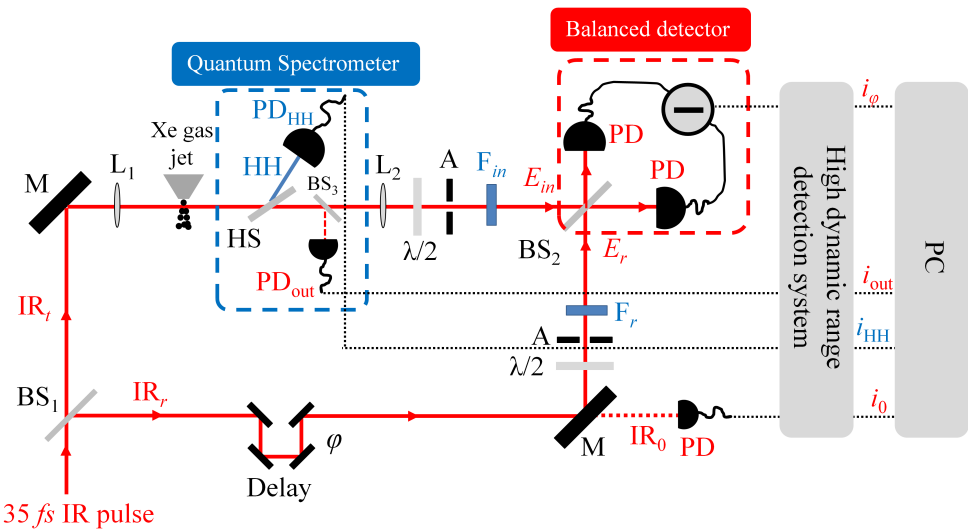


Figure 4: Optical layout of the experimental set-up. BS₁: 80:20 (Transmission:Reflection) IR beam splitter. IR_t: IR beam passing through BS₁. IR_r: IR beam reflected by BS₁. M: IR plane mirrors. L_{1,2}: Lens. HS: harmonic separator which reflects the high-harmonics and leaves the IR beam to pass through. HH: High-harmonics. BS_{2,3}: 50:50 IR beam splitter. PD, PD₀, PD_{out}, PD_{HH}: IR and HH photodetectors. PD₀ is part of the quantum spectrometer approach. λ/2: Half-IR-wave plate. A: Aperture. F_{in,r}: Neutral density filters. E_r is the local oscillator laser field of the reference beam and E_{in} is the light field to be characterized. i , i_{out} , i_0 , i_{HH} , are the photocurrent values recorded for each laser shot by a multichannel 16 bit high dynamic range boxcar integrator. For each shot the background electronic noise was recorded and subtracted by the corresponding photocurrent signal. The values were saved and analyzed by computer (PC) software.

process from all other processes induced by the interaction. Detailed description of the QS approach can be found in refs. (15, 16) of the main text of the manuscript. The IR beam exiting the QS was collimated by a concave lens (L_2) and its mean photon number was reduced by means of neutral density filters (F_{in}). The outgoing from the filters field (E_{in}) was spatiotemporally overlapped on a 50:50 beam splitter (BS_2) with an unaffected by the interaction local oscillator laser field (E_r) coming from the 2nd branch of the interferometer which consists a delay stage that introduces a controllable delay $\delta\tau$ (phase shift ϕ) between the E_r and E_{in} fields. The delay stage was consisting a rough precision steeper motor (supporting a displacement down to ≈ 20 nm per step) that has been used to temporally overlap and find the zero delay ($\delta\tau \approx 0$) of the E_r and E_{in} fields, and a high precision piezo based stage (supporting a displacement down to ≈ 2 nm per step) that has been used to record the field quadrature around $\delta\tau \approx 0$. The power of the E_r was controlled by means of neutral density filters (F_r). The F_{in} and F_r were mounted on a motorized translation stages. As the BS_2 is not perfectly insensitive to the polarization, the energy balance between the beams at the output of the BS_2 was adjusted by fine tuning (by the same angle) the $\lambda/2$ plates placed in each branch of the interferometer. In order to eliminate any wavefront imperfections that may appear along the beam profile of the interference fields, a pair of ≈ 2 mm diameter apertures (A) where placed in the beam paths selecting only the central part of the beam profiles. The outgoing from the BS_2 interfering fields were detected by the diodes (PD) of an high bandwidth (from DC to 350 MHz), high subtraction efficiency and high quantum efficiency, balanced amplified differential photodetector which provides at each value of ϕ the signal difference. The photocurrent difference i_ϕ as well as the photocurrent values of the IR and HH detectors (i_{out}, i_0, i_{HH}) in the QS, were simultaneously obtained for each laser shot by a multichannel 16 bit high dynamic range boxcar integrator. The photodiodes of the balanced detector were operating below their saturation threshold and its shot-noize power dependence in the linear regime. For each shot the background electronic noise was recorded and

subtracted by the corresponding photocurrent signal by placing a second time-gate in the boxcar integrator in times significantly delayed compared the arrival times light pulses. Care was taken to isolate/shield the interferometer, the electronics and the detectors from any environmental noises (mechanical/sound, electrical currents and photons). The experiment was remotely controlled in order to avoid introducing environmental noises during the measurements. A band block frequency filter operating in the range from 5×10^{-3} Hz to 150 Hz eliminates the noise instabilities introduced in the interferometer by the vacuum pumps and environmental mechanical noises leaving practically unaffected the quantum noise fluctuations of the light state and the mean oscillation frequency of the photocurrent signal i_ϕ . To temporally overlap and find the zero delay ($\delta\tau \approx 0$) of the E_r and E_{in} fields their energy R ratio was set to be in the range of $\sim 10^{-2}$. Setting the stepper motor stage around $\delta\tau \approx 0$, the characterization of the quantum state (and the measurements shown in the main text of the manuscript) of light, was achieved by setting the R in the range of $\sim 10^{-7}$ and accumulating $\approx 10^5$ shots. The measurement was performed by moving the piezo from $\phi = 0 - \varepsilon$ to $\phi = 0 + \varepsilon$ (where $\varepsilon \approx \pi/8$). As no feedback control loop (that provides the absolute piezo position i.e. ε) was used, the calibration of the x-axis of the homodyne traces was achieved by corresponding to $\phi = 0$ and $\phi = \pi$ the maximum and minimum mean values of i_ϕ , respectively. The homodyne data were scaled according to the measured vacuum state quadrature noise. The Wigner functions have been reconstructed from the experimental data following methodology of ref. (17).